

Ground spreading dynamics during single droplet impact onto a free-standing cubic surface element

A. K. Geppert^{*1}, B. Weigand¹

¹Institute of Aerospace Thermodynamics, University of Stuttgart, Germany

^{*}Corresponding author: anne.geppert@itlr.uni-stuttgart.de

Abstract

In many technical applications the impact of a single droplet onto a dry, structured surface plays an important role. Hereby, the impact dynamics are often affected also by the wettability of the respective surface. In order to gain a better understanding of the complex interplay between surface structure and wettability, the basic process of single droplet impact onto a free-standing cubic surface element with varying surface wettability is investigated experimentally. High-speed visualization of the impact process is performed with the multi-perspective experimental facility in our laboratory [1]. The experimental parameter range covers cubic pillars with varying edge length (between 1 mm and 2.4 mm) and different surface wettabilities, multiple droplet diameters, impact velocities and two fluids, namely water and isopropanol. The focus of this work is on the effects of surface wettability and drop-pillar ratio \bar{L}_D on the evolution of the spreading factor $d^* = d_s/D_d$ over the duration of the impact process.

Introduction

Single droplet impact onto dry, structured surfaces plays an important role in many technical applications. In addition to the surface structure itself, also the wettability affects the impact outcome and especially the liquids spreading behaviour. For example, the cooling of micro-electronic devices requires a high surface wettability to enhance the heat transfer, i.e. a complete as possible coverage of the surface with the cooling liquid. On the other hand, self-cleaning surfaces have a very low surface wettability to completely repel liquids. In order to

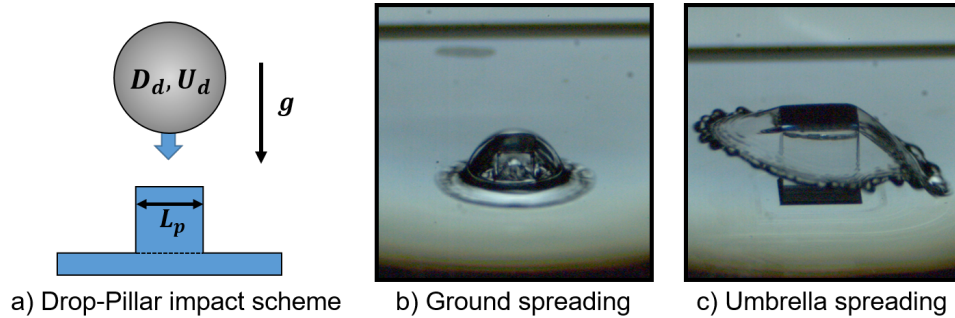


Figure 1. Schematic representation of droplet impact problem and observed impact morphologies.

gain a better understanding of the complex interplay between surface structure and wettability we investigated the basic process of droplet impact onto a free-standing cubic surface element (pillar) with varying surface wettability (see Fig. 1a). To begin with, the impact of an isopropanol droplet onto a pillar with 1 mm edge length, whose surface satisfied full wetting conditions, was studied with a combined numerical and experimental approach by Ren et al. [2]. It unraveled the process of air entrapment underneath the droplet and the subsequent bubble formation. Next, we expanded the parameter range to include additional pillar sizes (up to 2.4 mm) and surface wettabilities (characterized by the contact angle θ), multiple droplet diameters, impact velocities and a second test liquid (water). Defining the ratio of the pillar length L_p to the droplet diameter D_d as characteristic non-dimensional parameter $\bar{L}_D = L_p/D_d$ (pillar-drop ratio), we

could separate two different impact morphologies. For $\bar{L}_D = L_p/D_d < 1$, *ground spreading* occurs, i.e., the droplet liquid flows around the pillar, encloses it and spreads radially on the solid target surface (see Fig. 1b). If the pillar-drop ratio is $\bar{L}_D \gtrsim 1$, *umbrella spreading* takes place. In this case, the droplet spreading starts on top of the pillar and proceeds in mid-air (see Fig. 1c). A distinctive feature of umbrella spreading is the rectangular lamella, whose corners are azimuthally rotated by 45° with respect to the pillar corners.

The present investigation focuses on the detailed analysis of the spreading dynamics of the droplet, i.e. the temporal evolution of the spreading factor $d^* = d_s/D_d$ and its maximum value d_{max}^* . It includes a comparison to the spreading behaviour on smooth solid surfaces.

Experimental Facility

High-speed visualization of the impact process is performed with the multi-perspective experimental facility described in detail in Foltyn et al. [1]. The imaging systems records the droplet impact from four different perspectives (top, lateral, bottom and spatial view) and employs different imaging techniques, e.g. back-light imaging and total internal reflection method. The latter allows to clearly distinguish dry and wetted surface areas. The top, lateral and bottom views are recorded with two fully synchronized Photron SA-X2 cameras at a frame rate of 20,000 fps. The utilised optical resolutions are $17 \mu\text{m}/\text{px}$ (bottom), $18 \mu\text{m}/\text{px}$ (lateral) and $28 \mu\text{m}/\text{px}$ (top). The spatial view (see Fig. 1a,b) is recorded with a Chronos 1.4 colour camera at a frame rate of 1,000 fps and an optical resolution of $11 \mu\text{m}/\text{px}$. The droplet is generated by regular drip off from a tilted needle. Droplet diameters of 2.0 mm and 2.4 mm and impact velocities between 1.45 m s^{-1} and 3.35 m s^{-1} are used. Before impact, the droplet passes a laser light barrier, which triggers the image acquisition. The surface specimen, i.e. the free-standing pillars with edge length between 1 mm and 2.4 mm, are made of acrylic glass. The specimens wetting behaviour was manipulated with low pressure plasma activation (full wetting conditions, $\theta \approx 0^\circ$) and plasma polymerization (reduced wettability, $\theta \approx 71^\circ$; low wettability $\theta \approx 120^\circ$). Detailed information on the experimental facility and the post-processing procedures can be found in [1].

Results and Discussion

The investigated parameter space encompasses in total 65 experiments. Note that, in case of ground spreading d^* is derived from the bottom view images, while in case of umbrella spreading the top view images are used. The results focus on the effects of surface wettability and

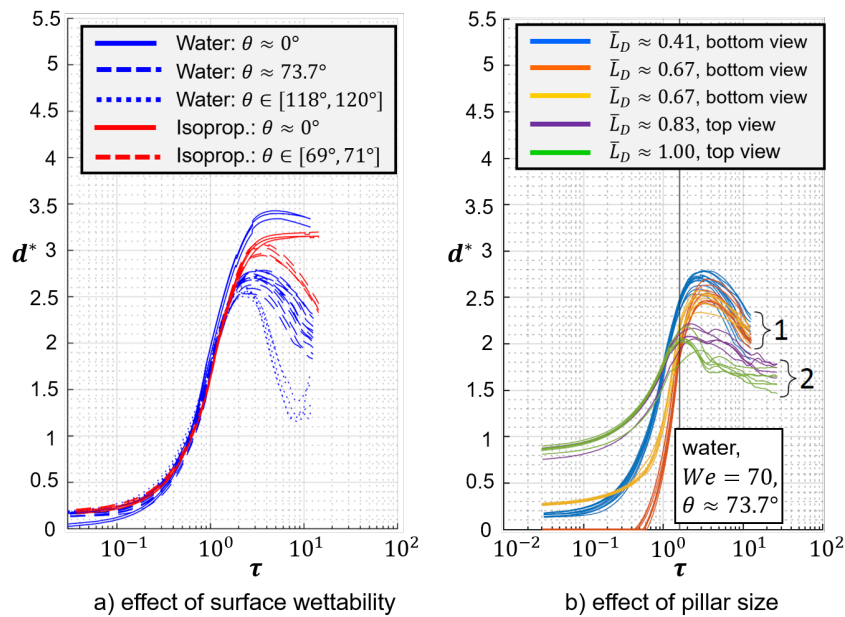


Figure 2. Temporal evolution of the spreading factor $d^* = d_s/D_d$.

drop-pillar ratio \bar{L}_D on the temporal evolution of the spreading factor $d^* = d_s/D_d$. In Figure 2a, the effect of surface wettability is shown for the smallest pillar size ($\bar{L}_D = 0.4 - 0.5$) and the lowest impact velocity, hence only ground spreading is observed. For a fully wettable surface (solid lines), the plateau phase follows directly after the kinematic and spreading phase defined by Rioboo et al. [3]. For the water droplet (blue) a slight receding of the liquid is observable, which is not the case for isopropanol. This results from the three times higher surface tension of water compared to isopropanol. With decreasing surface wettability (dashed lines), the droplet starts to recede immediately after reaching its maximum spreading diameter. In case of water droplet impact, d_{max}^* decreases strongly with decreasing surface wettability. A further decrease of surface wettability to hydrophobic conditions (dotted line) leads to an even faster droplet receding.

The effect of the drop-pillar ratio \bar{L}_D on the evolution of the spreading factor is shown in Figure 2b for water droplet impacts ($We = 70$) onto pillars with an intermediate surface wettability ($\theta \approx 73.7^\circ$). The curve progression of d^* over the non-dimensional time $\tau = tU/D_d$ can be directly related to the observed impact morphology. For the curves summarized with (1) ground spreading was observed. The droplet liquid flows around the pillar, encloses it and continues to spread radially on the solid target surface. After reaching d_{max}^* a receding motion is observed. The curves summarized with (2) represent umbrella spreading cases. Here d_{max}^* is smaller in comparison with the ground spreading cases and the receding motion slower, which results from the lamella spreading in air and not along a solid surface.

Conclusion

We experimentally investigated the droplet impact onto a free-standing cubic surface element with varying size and surface wettability. A change in impact morphology from ground spreading to umbrella spreading was observed when the pillar size is in the order of or larger than the droplet diameter. The temporal evolution of the spreading factor is strongly affected by both pillar size and surface wettability. To gain a better understanding of the effects a more detailed analysis will be conducted in the future.

Acknowledgments

The authors would like to thank the Deutsche Forschungsgemeinschaft (DFG) for the financial support of the project GRK 2160 "Droplet Interaction Technologies" (DROFIT), under project number 270852890.

Nomenclature

D_d	diameter of impacting droplet [m]
d_s	spreading diameter [m]
d^*	spreading factor, d_s/D_d [-]
d_{max}^*	maximum spreading factor, $d_{s,max}/D_d$ [-]
L_D	pillar edge length [m]
\bar{L}_D	drop-pillar ratio, L_p/D_d [-]
t	time [s]
U_d	velocity of impacting droplet [m/s]
θ	contact angle [$^\circ$]
τ	non-dimensional time, $(tU_d)/D_d$ [-]

References

- [1] P. Foltyn, D. Ribeiro, A. Silva, G. Lamanna, and B. Weigand. Influence of wetting behavior on the morphology of droplet impacts onto dry smooth surfaces. *Physics of Fluids*, 33(6):063305, 2021.
- [2] W. Ren, P. Foltyn, A. Geppert, and B. Weigand. Air entrapment and bubble formation during

- droplet impact onto a single cubic pillar. *Sci. Rep.*, 11(1):18018, 2021.
- [3] R. Rioboo, M. Marengo, and C. Tropea. Time evolution of liquid drop impact onto solid, dry surfaces. *Experiments in Fluids*, 33(1):112–124, 2002.